# RGB speckle pattern interferometry for surface metrology

Upputuri, Paul Kumar; Rajendran, Praveenbalaji; Pramanik, Manojit

2020

Upputuri, P. K., Rajendran, P., & Pramanik, M. (2020). RGB speckle pattern interferometry for surface metrology. Proceedings of SPIE - Quantitative Phase Imaging VI, 11249, 53-. doi:10.1117/12.2543916

https://hdl.handle.net/10356/146553

https://doi.org/10.1117/12.2543916

# RGB speckle pattern interferometry for surface metrology

Paul Kumar Upputuri*, Praveenbalaji Rajendran, and Manojit Pramanik
School of Chemical and Biomedical Engineering, Nanyang Technological University, Singapore 637459

**ABSTRACT**

Digital speckle pattern interferometry (DSPI) has been widely used for surface metrology of optically rough surfaces. Single visible wavelength can provide high measurement accuracy, but it limits the deformation measurement range of the interferometer. Also, it is difficult to reveal the shape of a rough surface with one wavelength in normal illumination and observation geometry. Using more than one visible wavelength in DSPI, one can measure large deformations as well as shape using synthetic wavelength approach. In this work, we will discuss multi-wavelength speckle pattern interferometry using a Bayer RGB sensor. The colour sensor allows simultaneous acquisition of speckle patterns at different wavelengths. The colour images acquired using RGB sensor is split in to its individual components and corresponding interference phase map is recovered using error compensating phase shifting algorithm. The wrapped phase is unwrapped to quantify the deformation or shape information of the sample under inspection. Theoretical background of RGB interferometry for deformation and shape measurements, and experimental results will be presented.

***Keyword*:** RGB interferometry, speckles, deformation, shape, phase shifting, colour CCD

## 1. INTRUDUCTION

Digital speckle pattern interferometry (DPSI) or TV holography (TVH) based on single wavelength configuration offers excellent resolution and high sensitivity for optical metrology applications [1-6]. DSPI system can study specimens under static, dynamic, or quasi-static loading [7, 8]. DSPI with phase shifting technique is well established for measurement of deformation and surface shape on both smooth and rough samples. Such systems are important in quality testing (functionality, reliability and integrity of the components) of Microsystems such as Micro-Electro-Mechanical Systems (MEMS) [9-13]. In 1λ-phase shifting interferometry (1λ-PSI), a serious limitation to their use is that the surface height/depth of less than half a wavelength only can be measured unambiguously[14]. The interferometric methods used to overcome such problems are: 2λ-phase shifting interferometry (2λ-PSI) [15-17], scanning white light interferometry (SWI)[18-20], spectrally resolved white light interferometry (SR-WLI) [21, 22], white light phase shifting interferometry[23-25], and 3λ-phase shifting interferometry (3λ-PSI) [26-28]. Single wavelength DSPI configuration suffers from overcrowding of fringes for large deflection that sets a limitation due to speckle de-correlation for quantitative phase analysis. And also, shape cannot be determined under normal illumination and observation condition (i.e. out-of-plane configuration), when single wavelength is used.

Multiple lasers have been used to overcome these drawbacks. Using two or three wavelengths in conventional DSPI, it is possible to reconstruct the shape of a rough surface even in out-of-plane configuration. Along with shape, deformation can also be measured at variable sensitivities using multiple wavelength techniques. Multiple wavelength techniques can be implemented in sequential illumination mode if monochrome camera [29], or in simultaneous illumination mode if colour camera is used [30]. In sequential illumination mode, images are acquired one by one, and hence it is a time consuming procedure and not suitable for dynamic measurements. Whereas in simultaneous illumination mode, images are acquired in one go. Conventional single-chip monochromatic CCD cameras can be used for sequential illumination method. For simultaneous recording of speckle or interference pattern a three-chip, Foveon X3 sensor or a single-chip colour CCD cameras is required [31]. If 3-CCD camera is used, there is no loss of spatial resolution, however, they are relatively expensive and needs skilled people for alignment. Due to these reasons, single chip colour camera is used for multiple laser interferometry, white light interferometry [32-34], etc. In this paper we demonstrate a red-green-blue (RGB) wavelength DSPI or TV holography for deflection measurements on rough surfaces using a single-chip colour CCD. The speckle patterns are stored simultaneously using a high resolution single-chip

* Email: paulkumaru@gmail.com

colour CCD camera. Thus the data acquisition procedure is as simple as single wavelength case. The colour RGB images are decomposed into its monochromatic components using software tools. An error compensating and higher order phase shifting algorithm [35] which is suitable for RGB wavelength analysis is used for phase evaluation at individual wavelengths. Theoretical background for deflection measurement and experimental results on deflection measured at effective wavelength using phase subtraction method are presented.

## 2. DEFORMATION MEASUREMENT USING PHASE SUBTRACTION METHOD - THEORETICAL BACKGROUND

If the test surface is rough, the interference between reference and test beams does not produce a visible fringe pattern. So, TV holography is used to study speckled surfaces. In TV holography, the intensity distributions of speckle patterns acquired before and after deformation are subtracted to generate speckle correlation fringes. The intensity distribution of speckle pattern before ($I^b$) and after ($I^a$) deformation can be written as

$$I^b = I_o(1 + V cos[\phi^b]) \tag{1}$$
$$I^a = I_o(1 + V \cos[\phi^b + \Delta\phi]) \tag{2}$$

where a, and b stand for after and before deformation, $\phi^b$ the random speckle phase, $\Delta\phi(= 4\pi w/\lambda)$ is the desired (deformation) phase, $w$ is the out-of-plane deformation. The subtraction of Eq.(1) from Eq.(2), results in deformation fringes [36]

$$\begin{aligned} |I^a - I^b| &= |I_o(1 + V \cos[\phi^b + \Delta\phi]) - I_o(1 + V cos[\phi^b])| \\ &= I_o V(cos[\phi^b + \Delta\phi] - \cos[\phi^b]) \end{aligned} \tag{3}$$

The intensity distribution of phase shifted frames before and after deformation at different wavelength can be written as [37]

$$I_{iN}^b = I_o\left(1 + V cos\left[\phi_i^b + (N-1)\alpha_i\right]\right) \tag{4}$$
$$I_{iN}^a = I_o(1 + V \cos[\phi_i^a + (N-1)\alpha_i]) \tag{5}$$

The phases before $\phi_i^b$and after $\phi_i^a(= \phi^b + \Delta\phi_i)$ deformation can be calculated using any one of the phase shifting algorithm. Using these phases, deformation and shape of the surface can be measured at different sensitivities. Once phases $\phi_i$ at different wavelengths are calculated using phase shifting algorithm (8-step algorithm), they can be subtracted to generate synthetic wavelength phases.

If $\Delta\phi_1$and $\Delta\phi_2$ are the deformation phases at two different wavelengths, $\lambda_1$ , and $\lambda_2$ then the deformation phase at synthetic wavelength can be generated by using the following equation [38, 39]

$$\Delta\phi_1 - \Delta\phi_2 = \frac{4\pi}{\Lambda} w \tag{6}$$

where $\Lambda = \lambda_1\lambda_2/|\lambda_1 - \lambda_2|$. The phase at synthetic wavelength reveals the deformation information at every point on the object surface. This approach enhances the measurement range by reducing the sensitivity of the system. The advantage is it can provide surface profile and shape simultaneously.

## 3. DESCRIPTION OF SPECKLE PATTERN INTERFEROMETRY SYSTEM WITH MULTIPLE WAVELENGTH ILLUMINATION

A multiple wavelength microscopic interferometry system is used for the deformation or deflection measurements on rough micro-specimens. The system is equipped with two lasers [a red laser, 632.8 nm and a green laser, 532 nm], a high-resolution colour CCD camera, and a microscope. If 632.8 nm and 532 nm are used for measurements, then the synthetic wavelength that can be generated is 3339.8 nm. The test sample was mounted under the microscope. The laser beams are expanded using a spatial filtering and collimated using a convex lens. Variable neutral density filters are used to control the intensity of individual laser beams. The collimated laser beams illuminate the microspecimen under study and a reference mirror via a beam splitter simultaneously. The microscopic imaging system consists of a microscope with an extended zoom range and a RGB colour camera. It is a color progressive scan camera with 5 million pixels resolution. These are single-chip colour sensors which contain the primary colours red, green, and blue and are used in most single-chip digital image sensors used in digital cameras to create a color image. It has 2456(H) X 2058(V) active pixels with a 3.45 µm square pixel. A PZT driven reference mirror is used for introducing the phase shifts between the object and reference beams. The scattered beam from the rough micro-specimen and the smooth beam from the reference mirror for each wavelength are recombined coherently onto the CCD plane. The interfeograms corresponding to each wavelength are recorded simultaneously using the colour CCD. The PZT is calibrated for known phase shift 90º for 532 nm wavelength. This will introduce a phase shift error at 632. 8 nm. To compensate for this error, a higher order phase shifting algorithm is used. Speckle patterns before and after loading the sample are subtracted to visualise the speckle intensity correlation fringes related to the deflection using software programs suitable for colour CCD camera. Also, phase shifted frames are stored in PC and analysed in for quantitative deflection information. Figure 1 shows the procedure to calculate effective wavelength deformation phase.

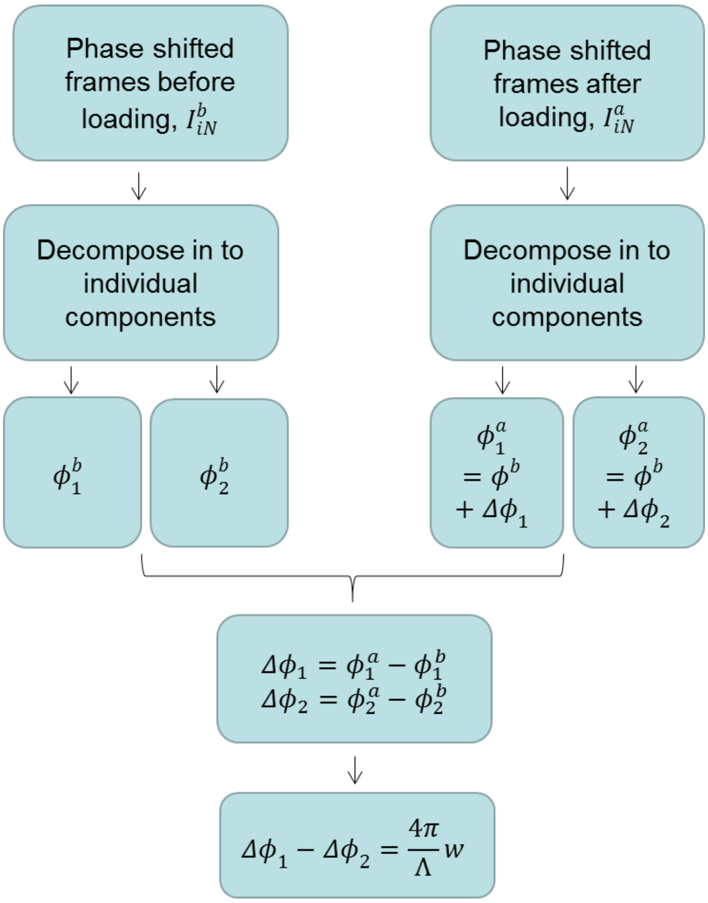


Fig. 1. Flow chart for the calculation of deformation phase at effective wavelength using simultaneously acquired phase shifted frames before and after loading the test sample. The colour images are decomposed in to in its individual components; here it is red and green.

## 4. MEASUREMENT OF MICRO-DEFORMATION ON ROUGH SURFACE

Initially, we have carried out experiments on a flat 1.5 X 2.0 mm$^2$ rough specimen. The test sample was mounted under the multiple-wavelength microscope equipped with two lasers and colour CCD. The red and green laser beams are simultaneously illuminated on the test surface and the reference mirror mounted on the PZT. The resultant speckle patterns are recorded by the colour CCD camera interfaced with the PC. Phase shifted frames are recorded by shifting the PZT mirror. Following the simultaneous recording procedure, multiple phase shifted frames before and after tilting the specimen are stored in the PC. Figure.1 shows the procedure for multiple wavelength speckle fringe analysis for deformation measurement. The speckle pattern stored by simultaneously illuminating the object (before loading) with red and green wavelengths is shown in Figure 2(a). The pattern thus stored are then decomposed in to its monochromatic components i.e. red@632.8 nm and green @ 532 nm, which are shown in Figure 2(b) and 2(c), respectively. The speckle patterns at single wavelength before and after loading are subtracted to generate speckle correlation fringes and the correlation fringes at 632.8 nm is shown in Figure 2(d). Similarly, correlation fringes can be generated for all the phase shifted frames and phase can be calculated from them using phase shifting algorithm. This procedure is called phase of difference in which the resultant phase is effected by the random speckle noise.

We used difference of phases method where there the phase before and after deformation are subtracted to yield deformation phase. This phase is more accurate and is suitable for pure static loading. The speckles phases before and after loading the sample are calculated at red and green wavelength separately as shown in the flow chart in Figure 1. The speckle phase before loading the sample calculated at red wavelength is shown in Figure 3(a). Figure 3(b) is the deflection phase obtained by subtracting the phase before and after loading at red wavelength. Here the number of fringes generated on the surface is less, *i.e.,* small surface deflection, hence any one of the phase map (measured at red or green) can be used to measure the deflection of the sample. If the surface variation or curvature is large, *i.e.,* more number of fringes is expected. If single wavelength fails to quantify the data, then one can use effective phase evaluation method in such case. The wrapped phase map generated at red wavelength is unwrapped and quantified, which is shown in the Figure 3(c). The quantified deflection profiles measured at red and green wavelengths are compared in Figure 3(d). The profiles are similar and maximum deflection is same i.e. 2.2 micrometre. If the deflection is large, the deflection phases measured at red and green can be subtracted to yield effective wavelength phase, following the Equation (6).

Another MEMS pressure sensor sample with circular membrane at its centre was tested for deformation measurement using the system. Pressure was applied externally in a controlled manner to deflect the membrane. The membrane was illuminated with red and green wavelengths simultaneously. Before applying the pressure, multiple phase shifted frames were recorded and similarly after applying the static pressure frames were acquired. Figure 4(a) is the wrapped phase of deflected membrane at red wavelength whereas Figure 4(b) is the wrapped phase at green wavelength. Even though the deflection was same, the fringe density in these two phase maps is different. The green wavelength phase has more number of fringes due to the wavelength difference. Green wavelength is about 100 nm shorter than the red wavelength. Shorter wavelength show high sensitivity for deflection measurement. Here the sensitivity of single wavelength system is half of the wavelength i.e. 266 nm for 532 nm. However, to characterize the pressure sensor under large loading single wavelength data may not be sufficient. Because at large loading, the deflection and hence the fringe density is more. In such cases, measuring the deflection accurately with single wavelength may be difficult. So the two wavelength data will help to increase the measurement range by reducing the sensitivity of the system. The deflection phase maps at red and green wavelengths are subtracted to generate wrapped phase at effective wavelength, which is 6.28 times longer than the 532 nm wavelength. The effective wavelength phase is shown in Figure 4(c). The sensitivity of this measurement is about 1.67 micrometre.

## 5. CONCLUSIONS

A multiple wavelength speckle pattern interferometry system was demonstrated for nano- to micro-deflection measurements on rough surfaces. Using single visible wavelength in interferometry can provide high accurate and high sensitive measurements. Using two-wavelength phase subtraction, measurement range can be extended to several microns depending on the choice of the two wavelengths. In implementing this approach, one of the major constraints is selection of closely neighboring wavelengths. If the two wavelengths are widely spaced, the effective-wavelength and hence the measurement range is reduced. The setup can be used to work at single wavelength, giving a very sensitive measurement with a limited range, or with multiple wavelengths, giving less sensitive measurements with an extended range. Interference patterns at all the wavelengths are recorded simultaneously using color CCD camera which makes the data acquisition process faster than the case when monochromatic camera (requires sequential illumination) is used. Thus the data acquisition and phase evaluation procedures are as simple as in case of single wavelength method. It also offers great flexibility in sensitivity and measurement range by an appropriate choice of the different wavelengths.

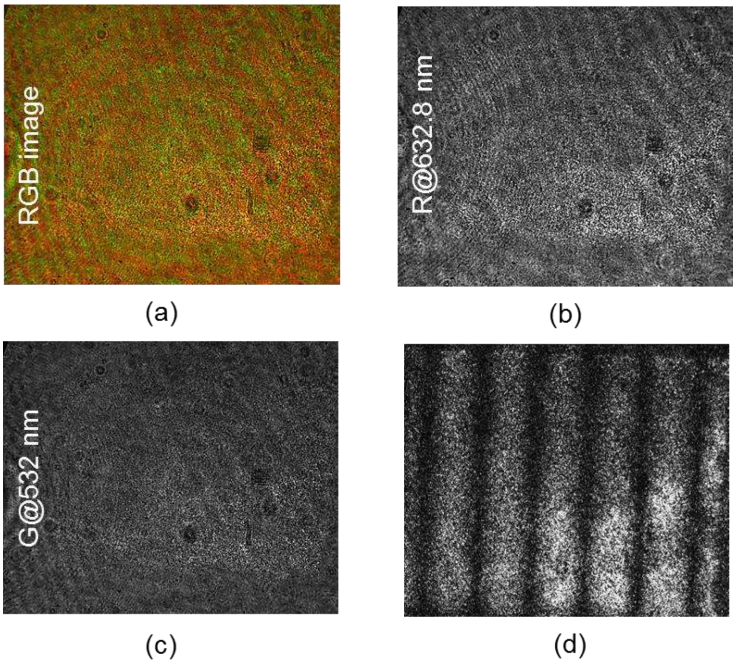


Fig. 2. Generation of speckle correlation fringes in multiple wavelength speckle pattern interferometry: (a) colour speckle pattern obtained with red and green light, (b) decomposed speckle pattern corresponding to red, (c) decomposed speckle pattern corresponding to green, and (d) deflection correlation fringes generated after subtracting the speckle pattern before and after deflection at red wavelength.

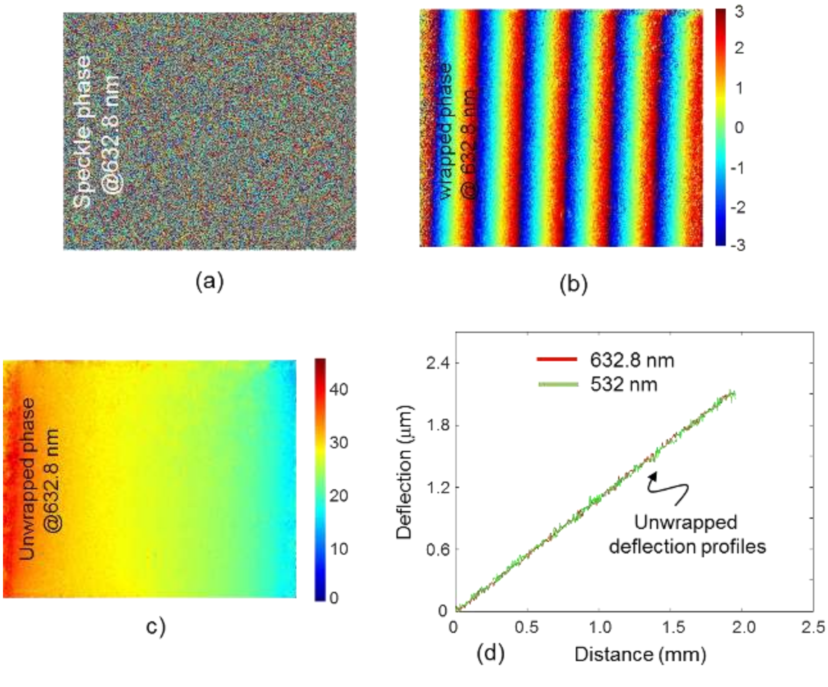


Fig. 3. Deflection phase analysis: (a) wrapped phase map at red before tilting the sample, (b) wrapped phase map obtained after subtracting the phase before and after tiling the sample at red wavelength, (c) unwrapped phase of the tilted sample at 632.8 nm, and (d) Unwrapped profiles measured at red and green wavelengths. The deflection profiles are similar at both the wavelengths.

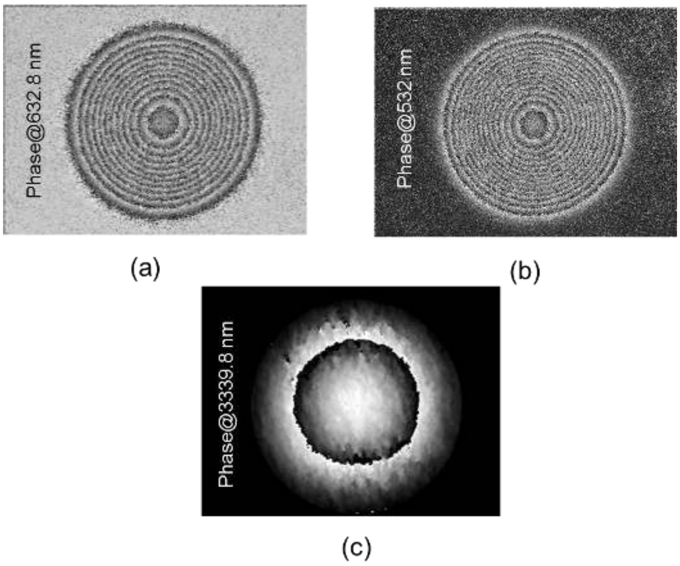


Fig. 4. Effective-wavelength deformation analysis on a MEMS circular pressure sensor: (a) deformation phase measured at red wavelength, (c) wrapped phase at green wavelength, and (c) effective wavelength phase obtained after subtracting two single wavelength phases. Here the sensitivity is reduced to about 1670 nm from 266 nm if 532 nm is used.

## ACKNOWLEDGMENT

The authors would like to acknowledge the financial support from the Singapore Ministry of Health's National Medical Research Council (NMRC/OFIRG/0005/2016: M4062012) and Tier 1 grant funded by Ministry of Education Singapore (RG144/18: M4012098).

## REFERENCES

[1] W. Steinchen, and L. Yang, "Digital Shearography: Theory and Application of Digital Speckle Pattern Shearing Interferometry," SPE Press ,Washington DC, PM100 (2003).
[2] U. P. Kumar, U. Somasundaram, N. K. Mohan *et al.*, "Comparative study of time average and stroboscopic illumination techniques for vibration fringe analysis," Journal of Optics, 40(4), 184-192 (2011).
[3] P. K. Rastogi, [Digital speckle pattern interferometry and related techniques] Wiley, New York(2001).
[4] P. K. Upputuri, K. M. Nandigana, and M. P. Kothiyal, "Single-shot interferometry techniques for optical testing," Asian Journal of Physics, 24, 1317-1338 (2015).
[5] P. J. de Groot, "A review of selected topics in interferometric optical metrology," Rep Prog Phys, 82(5), 056101 (2019).
[6] U. Paul Kumar, S. Pal, U. Somasundaram *et al.*, "Television (TV) Holography for Three-dimensional Surface Shape Measurement," Lasers in Engineering, 21, 231-240 (2011).
[7] U. Paul Kumar, N. Krishna Mohan, and M. P. Kothiyal, "Measurement of static and vibrating microsystems using microscopicTV holography," Optik - International Journal for Light and Electron Optics, 122(1), 49-54 (2011).
[8] U. P. Kumar, Y. Kalyani, N. K. Mohan *et al.*, "Time-average TV holography for vibration fringe analysis," Applied Optics, 48, 3094-3101 (2009).
[9] D. Grigg, E. Felkel, J. Roth *et al.*, "Static and dynamic characterization of MEMS and MOEMS devices using optical interference microscopy," Proceedings of SPIE, 5455, 429-435 (2004).
[10] U. P. Kumar, N. K. Mohan, and M. P. Kothiyal, "Characterization of micro-lenses based on single interferogram analysis using Hilbert transformation," Optics Communications, 284(21), 5084-5092 (2011).
[11] K. Creath, J. Burke, J. Schmit *et al.*, "Interferometric microscope with true color imaging," 9203, 92030S (2014).

[12] U. P. Kumar, N. K. Mohan, and M. P. Kothiyal, “Microscopic TV sherography for microsystems characterization,” Proceedings of SPIE, 7432, 74320T (2009).
[13] U. P. Kumar, U. Somasundaram, M. P. Kothiyal *et al.*, “Microscopic TV Holography for Microsystems Metrology,” Defence Science Journal, 61(5), (2011).
[14] P. K. Upputuri, L. Gong, H. Wang *et al.*, “Measurement of large discontinuities using single white light interferogram,” Opt Express, 22(22), 27373-80 (2014).
[15] P. K. Upputuri, M. Pramanik, M. P. Kothiyal *et al.*, "Two-wavelength microscopic speckle interferometry using colour CCD camera." 9302, 93023K.
[16] Q. Liu, L. Li, H. Zhang *et al.*, “Simultaneous dual-wavelength phase-shifting interferometry for surface topography measurement,” Optics and Lasers in Engineering, 124, (2020).
[17] P. K. Upputuri, S. Umapathy, M. Pramanik *et al.*, “Use of two wavelengths in microscopic TV holography for non destructive testing,” Optical Engineering, 53, 110501 (2014).
[18] F. Fang, Z. Zeng, X. Zhang *et al.*, “Measurement of micro-V-groove dihedral using white light interferometry,” Optics Communications, 359, 297-303 (2016).
[19] Z. Lei, X. Liu, L. Chen *et al.*, “A novel surface recovery algorithm in white light interferometry,” Measurement, 80, 1-11 (2016).
[20] B. Maniscalco, P. M. Kaminski, and J. M. Walls, “Thin film thickness measurements using Scanning White Light Interferometry,” Thin Solid Films, 550, 10-16 (2014).
[21] M. P. Kothiyal, and P. K. Upputuri, “Interferometry with broadband light: Applications in Metrology,” Asian Journal of Physics, 24(10), In Press (2015).
[22] P. Sandoz, G. Tribillon, and H. Perrin, “High-resolution profilometry by using phase calculation algorithms for spectroscopic analysis of white-light interferograms,” Journal of Modern Optics, 43(4), 701-708 (1996).
[23] P. K. Upputuri, M. Pramanik, K. M. Nandigana *et al.*, “White light single-shot interferometry with colour CCD camera for optical inspection of microsystems,” Proceedings of SPIE, 9524, 95240C (2015).
[24] J. C. Wyant, “White light interferometry ” Proceedings of SPIE, 4737, 98-107 (2002).
[25] T. Guo, F. Li, J. Chen *et al.*, “Multi-wavelength phase-shifting interferometry for micro-structures measurement based on color image processing in white light interference,” Optics and Lasers in Engineering, 82, 41-47 (2016).
[26] A. Pförtner, and J. Schwider, “3λ-Metrology,” Proceedings of SPIE, 4777, 194-201 (2002).
[27] A. D. Davies, J. Burke, K. Creath *et al.*, [Single-shot RGB polarising interferometer], (2018).
[28] U. Paul Kumar, N. Krishna Mohan, and M. P. Kothiyal, “Multiple wavelength interferometry for surface profiling,” Proceedings of SPIE, 7063, 70630W (2008).
[29] U. P. Kumar, N. K. Mohan, M. P. Kothiyal *et al.*, “Deformation and shape measurement using multiple wavelength microscopic TV holography,” Optical Engineering, 48(2), 023601 (2009).
[30] U. P. Kumar, N. K. Mohan, and M. P. Kothiyal, “Red-Green-Blue wavelength interferometry and TV holography for surface metrology,” Journal of Optics, 40(4), 176-183 (2011).
[31] P. K. Upputuri, M. Pramanik, K. M. Nandigana *et al.*, “Multi-colour microscopic interferometry for optical metrology and imaging applications,” Optics and Lasers in Engineering, 84, 10-25 (2016).
[32] M. Schake, and P. Lehmann, “Quadrature-based interferometry using pulsed RGB illumination,” Opt Express, 27(11), 16329-16343 (2019).
[33] P. K. Upputuri, M. Pramanik, K. M. Nandigana *et al.*, "White light single-shot interferometry with colour CCD camera for optical inspection of microsystems." 9524, 95240C.
[34] C. Gorecki, P. Lehmann, and M. Schake, [Perturbation resistant RGB-interferometry with pulsed LED illumination], (2018).
[35] J. Schmit, and K. Creath, “Extended averaging technique for derivation of error-compensating algorithms in phase-shifting interferometry,” Applied Optics, 34, 3610-3619 (1995).
[36] D. Malacara, [Optical Shop Testing] John Wiley & Sons, Inc., 674-763 (2007).
[37] U. Paul Kumar, B. Bhaduri, N. Krishna Mohan *et al.*, “Microscopic TV holography for MEMS deflection and 3-D surface profile characterization,” Optics and Lasers in Engineering, 46(9), 687-694 (2008).
[38] C. Polhemus, “Two-Wavelength Interferometry,” Applied Optics, 12, 2071-2074 (1973).
[39] Y.-Y. Cheng, and J. C. Wyant, “Multiple-wavelength phase-shifting interferometry,” Applied Optics, 24, 804-807 (1985).